IMPACT ASSESSMENT ON PEOPLE AND BUILDINGS FOR HYDROGEN PIPELINE EXPLOSIONS

Russo, P. [1], De Marco A.[1], Parisi F.[2]

[1] Department of Chemical Engineering, Materials and Environment, Sapienza University of Rome, via Eudossiana 18, 00184 Rome, Italy. email: paola.russo@uniroma1.it
[2] Department of Structures for Engineering and Architecture, University of Naples Federico II, via Claudio 21, 80125 Naples, Italy. email: fulvio.parisi@unina.it

ABSTRACT

Hydrogen has the potential to act as the energy carrier of the future. It will be then produced in large amounts and will certainly need to be transported for long distances. The safest way to transport hydrogen is through pipelines. Failure of pipelines carrying gaseous hydrogen can have several effects, some of which can pose a significant threat of damage to people and buildings in the immediate proximity of the failure location. This paper presents a probabilistic risk assessment procedure for the estimation of damage to people and buildings endangered by high-pressure hydrogen pipeline explosions. The procedure provides evaluation of annual probability of damage to people and buildings under an extreme event as a combination of the conditional probability of damage triggered by an explosion and the probability of occurrence of the explosion as a consequence of the pipeline failure. Physical features, such as the gas jet release process, flammable cloud size, blast generation, and explosion effects on people and buildings are considered and evaluated through the SLAB integral model, TNO model, Probit equations and Pressure-Impulse diagrams. For people, both direct and indirect effects of overpressure events are considered. For buildings, a comparison of the damage to different types of buildings (i.e. reinforced concrete buildings and tuff stone masonry buildings) is made. The probabilistic procedure presented may be used for designing a new hydrogen pipeline network and will be an advantageous tool for safety management of hydrogen gas pipelines.

INTRODUCTION

The growing demand for energy and the depletion of traditional energy sources, added to the need for increasing sustainable development in order to reduce environmental pollution, have made hydrogen a possible protagonist in today's society. Hydrogen represents an inexhaustible source, as an energy carrier, since it can be produced from different sources, both traditional and alternative ones. In addition, hydrogen plays a key role for sustainable development due to the fact that its combustion does not produce any pollution substances, especially greenhouse gases that contribute to an increase in global temperature.

Regarding hydrogen production, the production plant distribution in the World is shown in Table 1 [1]. Medium and large plants are distributed in several countries, with a maximum capacity of 290,000 Nm^3/h in Californian plant, and serve various type of industries (i.e. chemicals, petrochemicals, food, oil refining). Data reported in Table 1 refer to the existing and operating facilities (updated in January 2016), but more frequently investments in this alternative energy source are spreading. Recently, Linde's Global Hydrogen Business has announced that they will construct a $250 million world-scale hydrogen plant in Louisiana, with a production capacity of over 190,000 Nm^3/h, that will come on stream in 2021. The new plant will be part of Praxair's hydrogen system in Louisiana [2]. Growing investments have been made also in Europe over the last few years with an increase in the total production capacity from 17.799 Million Nm^3 in 2010 to 80.000 Million Nm^3 in 2017 [3]. In this framework, the increase of hydrogen production and distribution network is expected to increasingly grow the level of diffusion of this gas.

Large quantities of hydrogen from its production area to its utilization area are transported via dedicated pipelines. All over the World H_2 pipelines reach a total length of 4542 km, most of which

(2608 km) are located in the USA and some more (1598 km) in Europe, and only a small part (337 km) in the rest of the world (data updated to 2016) [4]. Nowadays, H_2 pipelines are mainly located in industrial areas, so their breakage may cause significant risk to the surrounding environment and the exposed people [5]. Therefore, the risks associated with a possible breakage of a pipeline carrying gaseous hydrogen must be taken into careful consideration. Consequences of gaseous hydrogen pipelines accidents can cause rather serious damage to people and buildings located in proximity of the pipeline involved in the hazard.

Following an accidental release of gas, a flammable cloud of gas is formed that mixes it with air and can be immediately ignited giving a jet flame, or later generating either a flash fire or an explosion. In the case of a fire the worst hazard for people and buildings is the direct contact with flames and thermal radiation, while in the case of an explosion it is the impact of the blast wave [6, 7]. From the analysis of the literature, it results that, as consequence of a pipeline failure, the event with a higher frequency of occurrence is represented by an explosion [8].

Table 1. Hydrogen production plants

	Europe	**Asia**	**North America**	**Rest of the world**
Company	**Capacity (Nm^3/h)**			
Air Liquide	770,505	730,846	830,326	89,283
Air Products	258,038	419,694	3,279,494	5,200
Linde	657,129	223,258	542,218	105,051
Praxair	13,500	197,304	2,201,225	13,396
Deokyang	-	111,000	-	-
Hyundai- Wison	-	-	-	301,411
Others	58,860	57,761	49,672	-
Total	**1,758,031**	**1,739,863**	**6,902,934**	**514,341**

In previous works [9,10], a procedure to evaluate the potential direct damage to building structures due to high-pressure pipeline explosions has been proposed. The procedure has been applied to both natural gas and hydrogen pipelines. The probability of occurrence of an explosion event as a result of a pipeline breakage has been estimated, and the consequence of the explosion (overpressure and impulse) have been evaluated. To characterize the hydrogen jet release a one-dimensional integral model, SLAB model [11], has been used. SLAB simulates the atmospheric dispersion of releases, taking several external factors into account, i.e. temperature, humidity, atmospheric stability, wind velocity, surface roughness. A release rate model has been combined with this dispersion model and the resulted overpressure and impulse are calculated by means of the TNO Multi-Energy Method [12]. Blast damage to building structures has been assessed through pressure–impulse diagrams that define the blast capacity of the selected structural members, that is, their ability to resist against different types of blast loads.

In this work, the same procedure is applied to estimate both harm to people and building direct structural damage associated with high-pressure hydrogen pipeline explosions. Specifically, the analysis refers to transmission and gathering pipelines located in industrial and rural areas. For people both direct and indirect effects of blasts are considered in order to evaluate the annual probability of damage [7]. As a main direct effect, the damage to pressure-sensitive organs, such as lungs and ears, due to the sudden increase in pressure, is considered. Among indirect effects both the impact of the head and the whole-body due to whole-body displacement are considered. During whole-body displacement, indeed, blast overpressure and impulses interact with the body in such a manner that it is essentially picked up and translated. On the contrary, the damage due to flying fragments hitting someone's body, and due to the impact caused by a collapsed structure to people inside buildings is not evaluated. With regard to direct damage to structures attributable to an air blast it can take various forms. For example, it may deflect structural steel frames, collapse roofs, dish-in walls, shatter panels,

and break windows. Specifically, direct damage to both reinforced concrete (RC) columns and load-bearing masonry walls of buildings are considered. What is finally evaluated is a minimum safety distance between hydrogen pipelines and people. The procedure presented herein may be used either to design/assess new pipeline networks in industrial or rural areas and existing building assets.

METHODOLOGY

Blast hazard

The methodology used in the present work, and reported in detail elsewhere [9, 10], consists of the following steps:

- simulations of hydrogen jet release process and estimation of flammable cloud size through the SLAB one- dimensional integral model incorporating a release rate model;
- calculation of the energy released by the explosion and its effects in terms of peak overpressure and impulse by the TNO Multi-Energy Method [12];
- evaluation of the blast hazard function, Pr[E|R], that provides the probability of occurrence of the explosion E in the event that a pipeline breakage R takes place.

A C++ code was developed and incorporated within the SLAB one-dimensional integral model. The C++ code combines a release rate model (see equations (1) and (2)) with pipeline operation properties, source release properties, and site. The release rate was estimated assuming sonic flow through an orifice of a high-pressure pipeline, and steady state conditions, as follows:

$$Q = \frac{\frac{\pi d^2 \alpha}{4}\sqrt{\gamma \rho_0 P_0 (\frac{2}{\gamma+1})^{\frac{\gamma+1}{\gamma-1}}}}{\sqrt{1+(4\alpha^2 f_F \frac{L}{d})(\frac{2}{\gamma+1})^{\frac{2}{\gamma-1}}}} \quad (1)$$

where α is the ratio of the effective hole area to the pipe sectional area (dimensionless hole size), d is the pipe diameter, ρ_0 and P_0 are the stagnation density and pressure of gas at operating conditions, respectively, γ is the specific heat ratio of gas, f_F is the Fanning friction factor and L is the pipe length from the hydrogen supply station to the release point.
To take into account that hydrogen is at high-pressure, the real gas model proposed by Abel-Noble equation of state (Eq. 2) was considered in Eq.1:

$$z = 1 + \frac{b \rho_0}{R_{H2} T} \quad (2)$$

where z is the compressibility factor, b is the co-volume (7.69×10^{-3} m^3/kg), R_{H2} is the hydrogen gas constant (4124.24 J/kg/K) (i.e. the ratio of the universal gas constant R to the molecular mass of hydrogen) and T is the temperature.
The calculated release rate is then used as the input to SLAB. SLAB is a computer model that allows to describe gas dispersion in the atmosphere, following a release [11]. The model assumes a specific shape for the crosswind concentration profile of the released gas. The downwind variations of spatially crosswind average concentrations are then determined by using conservation equations (i.e. mass, momentum, energy and species) in the downwind direction only. The main simulation output is the time-averaged concentration, expressed as a volume fraction, in the downwind direction. SLAB takes into account the atmospheric conditions and the turbulence generated by mixing the gas with the air. But it cannot simulate the gas flow either around obstacles or over a complex terrain. As an advantage, compared to a CFD model, this model requires much less computational cost. The code determines the

cloud extent corresponding to various pipeline operation properties, source release properties and site features.

The code then evaluates the consequences (i.e. overpressure and impulse) caused by the vapour cloud explosion according to the TNO Multi-Energy Method [12]. Blast equations corresponding to blast charts are included in the model to determine the peak overpressure P_s and positive phase duration t_p from a family of equations (curves) relating a dimensionless overpressure to the combustion energy scaled distance. The 10 blast strength equations (corresponding to TNO Multi-Energy curves) consist of positive pressure and time duration as functions of distance. The explosion parameters P_s and t_p at a given distance r from the explosion source are calculated for blast strengths 6 e 9. Finally, the positive impulse I is evaluated by integrating the overpressure variation over the positive phase duration.

Simulations are run by varying the geometric and operating properties of the pipeline (i.e. pipeline diameter, operating pressure, temperature), the source release properties (e.g. hole diameter, length of the pipeline from the compression station, distance from the explosion source), the atmospheric conditions (e.g. wind velocity, Pasquill-Gifford atmospheric stability class), and explosive class in the range of values reported in Table 2. For assessing blast probability statistics data of operating properties of pipelines for H_2 transmission and gathering available from US Pipeline and Hazardous Materials Safety Administration [13] and from literature [14] are employed.

The failure frequency of hydrogen pipeline breaches per length of pipeline is obtained using information from the Air Liquide [15]. The value of 0.126/year per 1,000 km is assumed. Data from the European Gas Pipeline Incident Group (EGIG) [16] are used to determine the relative probability and therefore the frequency of the various breach sizes. It is defined as follows: a small breach is the one with diameter of the hole (d_{hole}) smaller than or equal to 0.02 m; a medium breach is the one with the diameter of the hole large than 0.02 m and smaller or equal to the diameter of the pipe, and rupture when the diameter of the hole is larger than pipe diameter. Referring to data shown in Table 2 one might assign small, medium and rupture breaches with relative probabilities of 48%, 39% and 13%, respectively.

Table 2. Simulations conditions.

Parameter	Assumption
Source type	Horizontal jet release
Temperature of source material, K	200
Continuous source duration, s	600
Source height, m	1
Concentration averaging time, s	30
Maximum downwind distance, m	300
Surface roughness height, m	0.003
Wind velocity, m/s	2 and 5
Height of wind measurement, m	10
Ambient temperature, K	283
Relative humidity, %	75
Pasquill atmospheric stability class	A, C, D, F
Pipeline diameter (d), m	0.1016 - 0.508
Operating pressure (P_0), kPa	649 - 12,800
Hole diameter (d_{hole}), m	0.02 - d
Pipeline length from the gas supply station to the release point (L), m	50 - 10,000
Distance from explosion center (r), m	10 - 2000
Explosive class	6 and 9

In the simulations, a horizontal jet release was assumed as the worst case scenario. The source material is a temperature (200 K), evaluated by SLAB as a function of specific heat ratio, atmospheric pressure, operating pressure and temperature, and at height (1 m) typical in industrial areas. Four different Pasquill atmospheric stability classes [17] denoted as A (extremely unstable), C (slightly stable), D (neutrally stable) and F (moderately stable) are considered at wind velocity of 5 and 2 m/s, assuming a wind direction parallel to the gas jet. For the application of the TNO Multi-Energy Method, two classes corresponding to unconfined explosions, with low (class 6) and high (class 9) ignition power, are considered [12].
The results of the simulations are classified into 17 classes of overpressure and 13 classes of impulse. These values of overpressure and impulse are used to estimate the blast damage to people (death and injuries) and on structural components of typical buildings: reinforced concrete columns and tuff stone masonry walls.

Blast damage to people

People involved in an explosion can suffer from harm due to the high level of overpressure. Several effects of overpressure and duration of the high-pressure (impulse) event on people must be taken into account. Direct and indirect effects are generally distinguished. On the one hand, pressure-sensitive organs (i.e. lungs and ears) can be damaged by a change in pressure [18]. On the other hand, a person can be indirectly involved in the explosion and suffer from indirect damage, such as the impact from projectiles generated by structure damage or collapse. In addition, people can be thrown away from overpressure, with possible subsequent impact [19]. All these effects must be considered in order to establish the risk to which a person involved in the explosion may be exposed. Generally, a harm criterion is used to transform the consequences of an accident into a probability of harm to people [20]. For people, the consequences of an accidental event can provoke damage in terms of injury or fatality.

The generally applied method to estimate the level of harm to people as a consequence of an explosion uses the Probit (Probability unit) Functions, which characterize the dose-effect relationship [19, 21, 22]. A Probit Function transforms a dose level (V) to a probability of injury or fatality. The Probit variable Y is evaluated through Equation 3 [22]:

$$Y = k_1 + k_2 \ln V \tag{3}$$

where k_1, k_2 are empirical constants that reflect the specific hazard and V is the causative factor that represents the dose. To convert Probits to percentage which is the probability of a specific damage, Equation 4 is used:

$$P = 50\left[1 + \frac{Y-5}{|Y-5|}\, erf\left(\frac{|Y-5|}{\sqrt{2}}\right)\right] \tag{4}$$

where erf is the error function. Probit functions are particularly useful in QRA since they can provide harm probabilities for the range of accidents included in risk assessment. Table 3 lists the Probit equations used in this work to calculate both death and injury to people.

In particular, for deaths from lung haemorrhage the correlation uses as the causative variable a combination of overpressure, impulse and dynamic pressure (P_{ef}) and mass of person [19]. For deaths from lung haemorrhage an overpressure threshold value of 82.7-103.4 kPa [23] and an impulse threshold value of 180 kPa ms [24] are reported in literature. For damage due to the whole-body displacement, the available correlation provides a probability of harm as a function of both the peak overpressure and the impulse [19]. Overpressure threshold values of 55.16 and 75.84 kPa, respectively, for deaths from head impact and whole-body impact are reported in [25-27] when people are knocked down by pressure waves. Finally, impulse threshold value of 370 kPa ms [24] is considered to cause 1% serious injury from displacement.

Table 3. Probit functions for damage caused by explosion.

Damage	Probit Equation
Deaths from lung haemorrhage	$Y= 5 – 5.74 \ln [4.2 P_a/P_{ef} +1.3/I_{sc}]^a$ [19]
Deaths from head impact	$Y= 5 – 8.49 \ln [2430/P_s +4 \times 10^8/P_s I]^b$ [19]
Deaths from whole body impact	$Y= 5 – 2.44 \ln [7380/P_s +1.3 \times 10^9/P_s I]^b$ [19]
Injuries from ear-drum rupture	$Y = –12.6+1.524 P_s^c$ [22]
a: P_a=atmospheric pressure [Pa], $I_{sc}=I/(P_o^{1/2} \times m^{1/3})$, m=mass of person =70 kg, P_s=peak overpressure [Pa], $P_{ef}=P_s+5 \times P_s^2/(2 \times P_s +1.4 \times 10^6)$, b: P_s=peak overpressure [Pa], I=impulse of the shock wave [Pa x s] c: P_s=peak overpressure [Pa]	

With regards to reversible damage, that only induces injuries, the most sensitive organ to pressure changes is the ear and the damage to hearing is brought about by the ear-drum rupture. The overpressure threshold value for ear-drum rupture is 13.8 kPa [23]. Flying fragments can also cause injuries which depend on the size and weight of fragments, the impact velocity and the location of the impact on a human body [19]. However, the lack of properly validated models makes it difficult to fully evaluate the impact of missiles on people [18].

Once the probability of fatalities and injuries for the various direct and indirect effects of the explosion has been evaluated, the annual probability of damage to people under the explosion event is then calculated. It is a combination of the conditional probability of damage given by an explosion, *P[D|E]*, and the probability of occurrence of the explosion as consequence of pipeline failure, *P[E|R]*, and it is calculated as follows:

$$P\,[D] = P[D|E]P[E|R]\lambda_R \tag{5}$$

where *D* is the damage to people (death or injury); *E* is the explosion event; *R* is the pipeline rupture; λ_R is annual rate of pipeline rupture occurrence, year per 1,000 km. A value of 0.126/year per 1,000 km in Eq. 5 is used [15]. In the case of fatality *P[D|E]* is the cumulative probability of deaths from lung haemorrhage and whole-body displacement.

Blast damage to structural components

Pressure-impulse diagrams represent a powerful tool for safety verification of structures subjects to blast loading. They are capacity models that allow for several failure modes (e.g. flexural, shear, mixed flexural- shear) to be considered. Pressure-impulse diagrams define iso-damage curves that are the critical combinations of peak overpressure (P_s) and impulse (I) causing the same level of blast damage. This latter can be quantified through different damage measures (DMs), depending on the type of structural component and its expected failure modes.

After a DM is selected and a level of blast damage is defined through a DM value, the pressure-impulse diagram provides with a separation between safe and failure conditions, considering three regions of structural behaviour: quasi-static, dynamic, and impulsive loading. In quasi-static conditions, the pressure-time history of blast loading is characterized by very long duration with respect to the natural vibration period of the structural component, so failure occurs when the peak overpressure reaches the pressure asymptote. On the contrary, impulsive blast loads have very short duration, resulting in failure when the impulse attains the impulse asymptote. Dynamic blast loads produce a mixed structural response, so failure actually occurs if the peak overpressure and impulse define one of the critical combinations of the pressure-impulse diagram. The safety region corresponding to a prescribed performance of the structural component (and hence, damage level) is placed below the pressure-impulse diagram.

In this study, pressure-impulse capacity models are used to take into account the dynamic behaviour and failure modes of two different types of structural components: (i) reinforced concrete (RC) columns of framed buildings, and (ii) tuff stone masonry (TSM) walls of ancient buildings.

Reinforced Concrete columns

The Pressure-Impulse diagrams for RC columns were evaluated by Parisi [27] on the basis of Monte Carlo simulations, accounting for uncertainties in structural capacity, including those associated with mechanical properties of concrete and reinforcing steel, geometrical properties of columns and steel reinforcement. Those diagrams are characterized by a uniform probability of failure, and are proposed for three levels of damage: minor damage; moderate damage and near collapse. In this work, the median pressure-impulse diagrams associated with a near collapse condition of RC columns are taken into account.

RC columns of gravity-load designed buildings are selected. The columns have the following properties: concrete strength class C20/25 typically used in Italian RC buildings after 1971 (where 20 and 25 indicate the cylinder and cube characteristic compressive strengths of concrete, respectively); steel type FeB44k (roughly corresponding to the current B450C), which is characterized by ribbed bars and squared cross section with size 300x300 mm^2. All columns are assumed to have a concrete cover c = 30 mm and nominal height H = 3.00 m, which is a typical inter-storey height in residential buildings

Tuff stones masonry walls

Load-bearing masonry walls are key structural components of masonry buildings. They are chosen because the blast resistance of such walls is strongly different from that of RC columns: the compressive strength of unreinforced masonry being significantly lower than that of concrete, the capability of withstanding tensile stresses being the same as in the case of steel reinforcement in RC members, response sensitivity to axial loading, and boundary conditions are different. Therefore, they typically suffer from flexural out-of- plane failure under blast loading.

TSM walls with height h_w = 3.00 m, slenderness ratio l = 10 and pre-compression level P_v/f_m = 25% are taken into consideration, where: l is the ratio between h_w and thickness t_w (which is thus assumed to be 300 mm herein); P_v is the average compressive stress due to gravity loads; and f_m is the peak compressive strength of masonry. The selected TSM walls have the following material properties: material density ρ=1360 kg/m^3; Poisson's ratio n = 0.25; Young's modulus E = 2159 MPa; and peak compressive strength f_m = 3.96 MPa.

In this study, selected Pressure-Impulse diagrams derived through nonlinear dynamic analysis of elastic finite element models with tie-break resisting force are selected according to a previous study [28].

RESULTS

The first results of the analysis are in terms of probability to achieve given values of overpressure and impulse during the explosion, *P[E|R]*. From a probabilistic standpoint, the highest values of peak overpressure and impulse corresponding to blast strength 9 were found to be 507 kPa and 60,000 kPa ms, respectively. In the case of strength 6, those maximum values reduced to 36 kPa and 4,500 kPa ms. It is also noted that the results are slightly influenced (differences below 10%) by the atmospheric conditions chosen for the simulations. Specifically, the stability class F with wind velocity of 2 m/s can be considered the worst case scenario at which the higher probability to achieve the maximum pressure and impulse corresponds, because, in being a moderately stable class, with a lower wind velocity, dispersion is slower. Therefore, in the following cases the results were reported just for this condition. Fig. 1a and b shows the Pressure-Impulse diagrams for the gravity-load RC columns and the TSM load-bearing walls, respectively. The individual points corresponding to the possible

combination of pressure and impulse reached by an explosion are within. The designed RC columns can be considered safe against hydrogen gas explosions, for the worst case scenario (explosive class 9 and atmospheric stability class F2) and hence for all the investigated explosive classes and atmospheric stability classes. On the contrary, TSM load-bearing walls show higher vulnerability to blast loading. Indeed, the values of pressure and impulse asymptotes that characterize the blast capacity of those masonry components with medium pre-compression level, i.e. 3.5 kPa and 455 kPa ms, are very low [29].

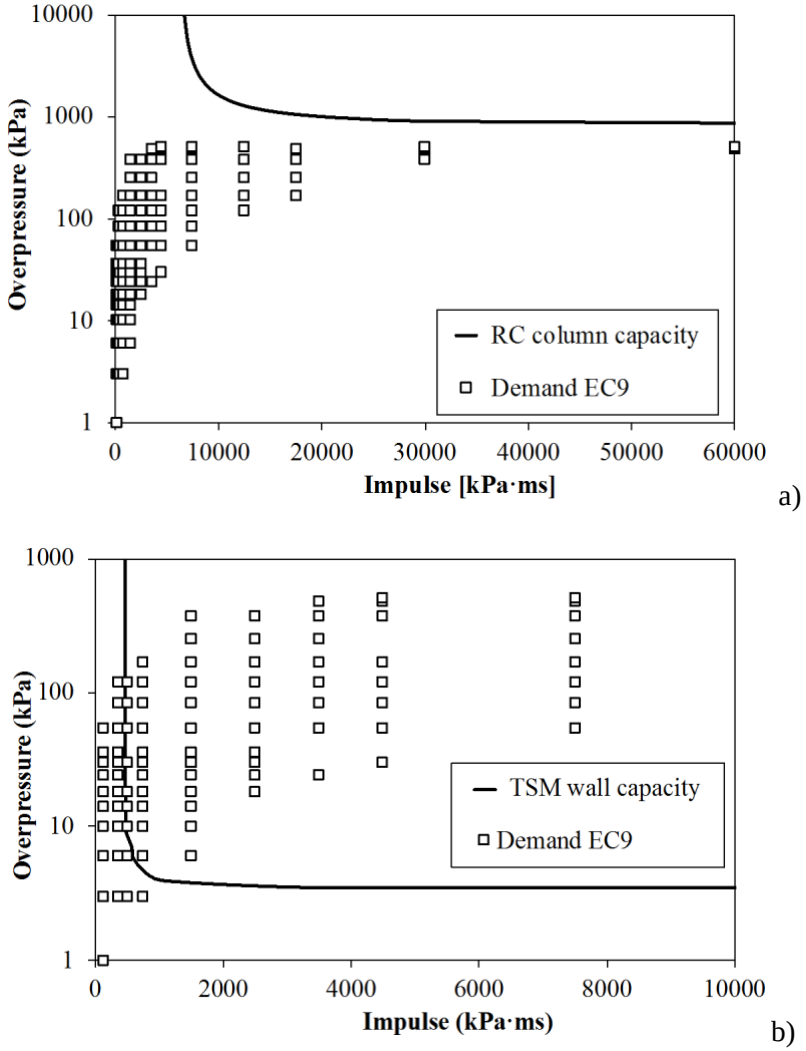

Figure 1. Comparison between blast demand and capacity of RC columns (a) and TSM walls (b) for explosive class 9 and atmospheric stability class F2.

With regards to the harm to people, probability of fatality from lung haemorrhage, head impact and whole body impact for the different overpressure-impulse values are reported in Figures 2-4, respectively. They refer to stability class F and wind velocity 2 m/s, and to explosive class 9.

Comparing Figures 2 to 4, the higher probability of fatality occurs from indirect effects such as from head and whole-body impact against obstacles. Indeed, the overpressures required to cause fatal lung damage are significantly higher than the values required to throw a person against obstacles. A maximum value of $1.65 \cdot 10^{-3}$ death/year/1000 km is obtained in the case of head impact for an explosion overpressure of 507 kPa and impulse of 12,500 kPa ms.

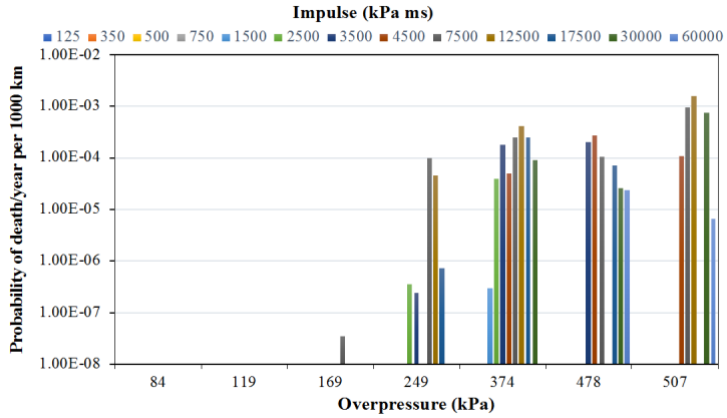

Figure 2. Probability of death from lung haemorrhage for explosive class 9 and atmospheric stability class F2.

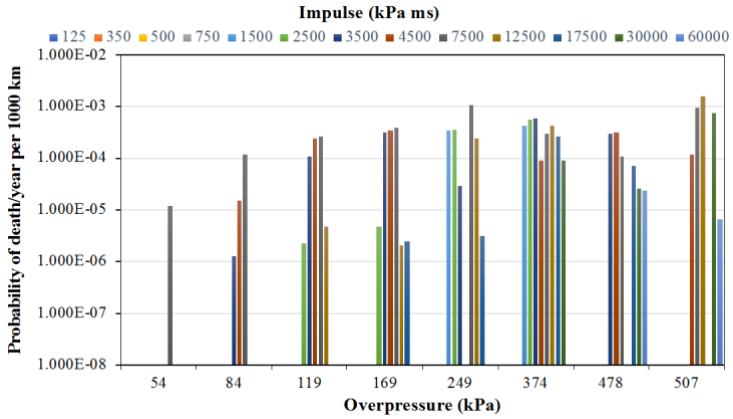

Figure 3. Probability of death from head impact for explosive class 9 and atmospheric stability class F2.

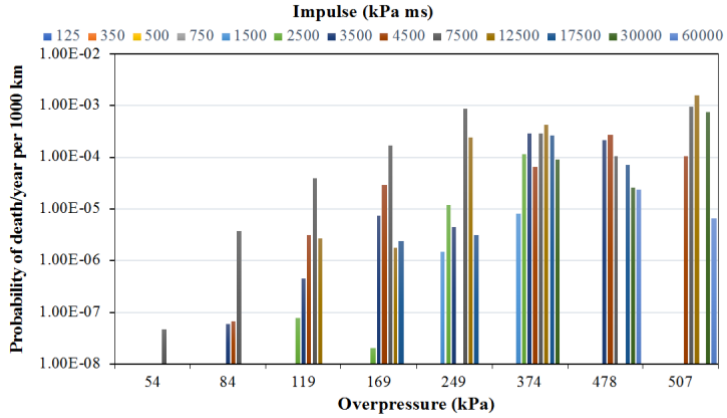

Figure 4. Probability of death from whole body impact for explosive class 9 and atmospheric stability class F2.

Once the risk related to the hazards is assessed the results are compared to acceptance criteria. If the results can meet these criteria the risk is defined acceptable. On the other hand, if the result does not meet the criteria possible mitigation measures should be evaluated. The selection and application of risk acceptance criteria for the hydrogen risk assessments reflects the general practice within risk assessments, and are also adapted to company and authority regulations. No adaptations to acceptance criteria have been made in order to reflect specificities of hydrogen technologies or operation of hydrogen facilities.

EIGA [30] defines the harm criteria as being approximately a 1% chance of individual risk of serious injury or fatality, and proposes the individual harm exposure threshold for determining safety distances of 3.5 x 10^{-5} per year. HSE has specified risk criteria to indicate the boundaries between the zones for hazards involving the risk of single or multiple fatalities. The individual risk criteria are [31]: maximum tolerable risk for workers 10^{-3} per year; maximum tolerable risk for the public 10^{-4} per year; broadly acceptable risk10^{-6} per year. Risks falling into the region below 10^{-6} per year are generally regarded as insignificant and adequately controlled. In the Netherlands, the maximum acceptable individual risk is 10^{-6} per year [31]. This is a statutory limit for "vulnerable objects" (i.e. housing, hospitals, schools etc), and a target to be achieved as far as possible for "less vulnerable objects" (i.e. shops, offices, recreational facilities). This applies equally to risks from fixed installations and transport of dangerous substances. It is calculated for an unprotected person (i.e. outdoors) present all year at specific locations. Therefore, in order to measure the risk levels for on-site personnel, and general public that may be exposed to the accidents originating from the hydrogen facilities the quantitative acceptance criteria considered are 10^{-6} per year [31].

From comparison with acceptance criteria the fatality risk is not acceptable in the case of explosive class 9, and atmospheric stability class F2. On the contrary, in the case of explosive class 6 and F2 the probability of death (10^{-11} death/year/1000 km) is well below the risk acceptance criteria.

With regards to injuries (Figure 5), since the overpressures required to cause eardrum rupture fatal lung damage are quite low, probability of injuries are higher than 10^{-5} /year/1000 km for overpressure higher than 10 kPa. Similar results were obtained also for explosive class 6 and the same atmospheric class F2.

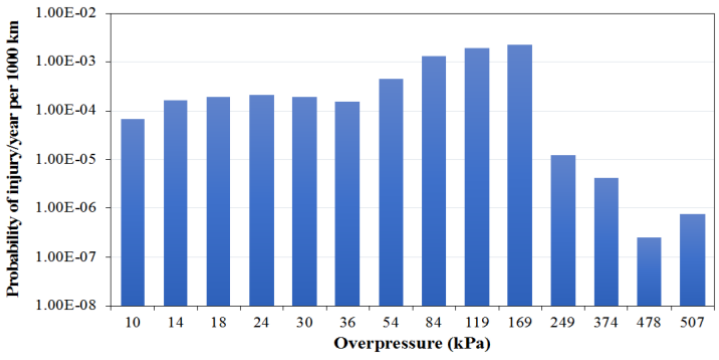

Figure 5. Probability of injury from eardrum rupture for explosive class 9 and atmospheric stability class F2.

Moreover, the extent of the damage to buildings depend on both the level of overpressure and impulse and the type of construction of structure. From the analysis carried out on reinforced concrete columns and tuff stone masonry walls, it is possible to conclude that there is no risk of harm in the case of reinforced concrete columns of framed buildings because those structural components do not collapse.

On the contrary, the higher vulnerability of TSM load-bearing walls to blast loading can cause indirect damage to the people inside the building.

Finally, a minimum safety distance between pipelines and populated area is derived. The safety distance is here considered as the minimum separation between a hazard source and a person, which will mitigate the effect of a likely foreseeable incident. The individual harm exposure threshold for determining safety distances is equal to 10^{-6} per year. From comparison with the harm criteria a safety distance of 500 m is calculated.

CONCLUSIONS

In this work, a probabilistic procedure to evaluate the damage to people and buildings involved in a gaseous hydrogen pipeline explosions has been applied. Probit equations have been used to evaluate and quantify the level and type of harm on people. Both indirect and direct damage are taken into account. The main human organs suffering from sudden changes in pressure are lungs and ear-drums and damage to these organs has been examined. As a consequence of an explosion, people can also be thrown away by the blast wave, suffering damage due to head impact or whole-body displacement.

The highest probability of fatality occurs from indirect effects such as from head and whole-body impact against obstacles. A maximum value of $1.65 \cdot 10^{-3}$ death/year/1000 km is obtained in the case of explosive class with high ignition power (class 9) and stable atmospheric conditions (F2).

In addition, a person inside a structure would more likely be injured or killed by the facility collapse than from lung damage. The assessment of structural damage has shown very low levels of risk of damage to reinforced concrete columns of framed buildings, because those structural components do not collapse. On the contrary, the higher vulnerability of TSM load-bearing walls to blast loading can cause indirect damage to the people inside the building. A safe distance of 500 m has been proposed in order to design a new pipeline network.

REFERENCES

1. Merchdant Hydrogen Plant Capacities, available at https://h2tools.org/hyarc/hydrogen-production accessed on 20.03.2019
2. Linde Engineering News, available at https://www.linde-engineering.com/en/news_and_media/press_releases/news-20190228 accessed on 20.03.2019
3. Eurostat data of Statistics on the production of manufactured goods, available at http://ec.europa.eu/eurostat/web/main accessed on 20.03.2019
4. Hydrogen Pipelines, available at https://h2tools.org/hyarc/hydrogen-delivery accessed on 20.03.2019
5. Zhang X., Xiao L., Analysis of Hazardous Chemicals Transportation Accidents and Transportation Management, Chemical Engineering Transactions, 67, No. 1, 2018, pp. 745-750.
6. Rusin A., Stolecka K., Hazards Associated with Hydrogen Infrastructure, Journal of Power Technologies, 97, No. 2, 2017, pp.153-157.
7. Crowl D. A., Understanding explosions, 2003, American Institute of Chemical Enginers, New York.
8. Gerboni R., Salvador E., Hydrogen transportation system: elements of risk analysis, Energy, 34, No.1, 2009, pp. 2223-2229.
9. Russo P., De Marco A., Parisi F., Failure of concrete and tuff stone masonry buildings as consequence of hydrogen pipeline explosions, International Journal of Hydrogen Energy, 2019, in press.
10. Russo P., Parisi F., Risk-targeted safety distance of reinforced concrete buildings from natural-gas transmission pipelines, Reliability Engineering and System Safety, 148, 2016, pp. 57–66.
11. Ermak DL., SLAB an atmospheric dispersion model for denser than air releases (UCRL-MA-105607), Livermore: Lawrence Livermore National Laboratory, 1990.

12. TNO, Methods for the calculation of physical effects due to releases of hazardous materials (liquid and gases), Yellow book, van den Bosh, 2005, C.J. H., Weterings, R.A.P.M. (Eds) TNO, The Hague.
13. PHMSA, Gas Distribution, Gas Gathering, Gas Transmission, Hazardous Liquids, Liquefied Natural Gas (LNG) and Underground Natural Gas Storage (UNGS) Annual Report Data, Available https://www.phmsa.dot.gov/data-and-statistics/pipeline/gas-distribution-gas-gathering-gas-transmission-hazardous-liquids, accessed on 16.06.2018.
14. Bedel L., Junker M., Natural gas pipelines for hydrogen transportation, Proceedings of 16th World Hydrogen energy Conference 2006 (WHEC 2006), 13-16 June 2006, Lyon, France, ISBN:9781622765409, 1006-1010.
15. Air Liquide, Questions and Issues on Hydrogen Pipelines, Pipeline Transmission of Hydrogen, Doe Hydrogen Pipeline Working Group Meeting, August 31, 2005, available at https://www.energy.gov/sites/prod/files/2014/03/f10/hpwgw_questissues_campbell.pdf accessed on 20.03.2019
16. EGIG, 8th Report of the European Gas Pipeline Incident Data Group. Groningen: European Gas Pipeline Incident Data Group, 2011.
17. Pasquill F., The estimation of the dispersion of windborne material, Meteorological Magazin, 90, 1961, pp.33-49.
18. HyResponse, Grant agreement No: 325348, Compiled by S. Tretsiakova-McNally; reviewed by D. Makarov (Ulster University), Lecture-Harm criteria for people and environment, damage criteria for structures and equipment, 2016.
19. TNO, Methods for the determination of possible damage, Green Book, 1989, In: CPR 16E., The Netherlands Organization of Applied Scientific Research.
20. LaChance J., Tchouvelev A., Engebo A., Development of uniform harm criteria for use in quantitative risk analysis of the hydrogen infrastructure, International Journal of Hydrogen Energy, 36, No. 3, 2011, pp. 2381-2388.
21. HSE, *Methods of approximation and determination of human vulnerability for offshore major accident hazard assessment*. UK 2010 SPC/Tech/OSD/30, rev 2013.
22. Crowl D.A., Louvar J., Chemical process safety fundamentals with applications, 2011, 3rd, ed. Prentice Hall, Upper Saddle River.
23. Jeffries R.M., Hunt S.J., Gould L., Derivation of fatality of probability function for occupant buildings subject to blast loads, Health & Safety Executive, 1997.
24. NFPA, NFPA 2, Hydrogen Technologies Code, Quincy, MA 02169-7471, NFPA 2, 2011.
25. AIChE Center for Chemical Process Safety, Guidance for Consequence Analysis of Chemical Releases, Center for Chemical Process Safety, American Institute of Chemical Engineers, New York: American institute of Chemical Engineers, 1999.
26. CCPS, Guidelines for Evaluating the Characteristics of Vapour Cloud Explosions, Flash Fires and BLEVEs, New York: American institute of Chemical Engineering, 1994.
27. Federal Emergency Management Agency, Handbook of Chemical Hazard Analysis Procedures, Washington, D.C., 1987.
28. Parisi F., Blast fragility and performance-based pressure- impulse diagrams of European reinforced concrete columns. Engineering Structures,103, 2015, pp.285-297.
29. Parisi F, Balestrieri C, Asprone D., Blast resistance of tuff stone masonry walls, Engineering Structures 113, 2016; pp. 233-244.
30. EIGA, European Industrial Gases Association, Determination of safety distances, IGC Doc 75/07/E, Revision of Doc 75/01/rev, 2007.
31. DNV, Risk Acceptance Criteria and Risk Based Damage Stability. Final Report, part 1: Risk Acceptance Criteria: Report no.: 2015-0165, Rev 2, 2015.